



Calibrating the camera for the First G-APD Cherenkov Telescope (FACT)

T. KRÄHENBÜHL¹, H. ANDERHUB¹, M. BACKES², A. BILAND¹, A. BOLLER¹, I. BRAUN¹, T. BRETZ³, V. COMMICHAU¹, L. DJAMBAZOV¹, D. DORNER⁴, C. FARNIER⁴, A. GENDOTTI¹, O. GRIMM¹, H.P. VON GUNTEN¹, D. HILDEBRAND¹, U. HORISBERGER¹, B. HUBER^{1a}, K.-S. KIM^{1b}, J.-H. KÖHNE², B. KRUMM², M. LEE^{1b}, J.-P. LENAIN⁴, E. LORENZ^{1c}, W. LUSTERMANN¹, E. LYARD⁴, K. MANNHEIM⁵, M. MEHARGA⁴, D. NEISE², F. NESSI-TEDALDI¹, A.-K. OVERKEMPING², F. PAUSS¹, D. RENKER^{1d}, W. RHODE², M. RIBORDY³, R. ROHLFS⁴, U. RÖSER¹, J.-P. STUCKI¹, J. SCHNEIDER¹, J. THAELE², O. TIBOLLA⁵, G. VIERTEL¹, P. VOGLER¹, R. WALTER⁴, K. WARDA², Q. WEITZEL¹

¹ETH Zurich, Institute for Particle Physics, Schafmattstrasse 20, CH-8093 Zurich, Switzerland

²Technische Universität Dortmund, Experimental Physics 5, Otto-Hahn-Str. 4, D-44221 Dortmund, Germany

³École Polytechnique Fédérale de Lausanne, Laboratory for High Energy Physics, CH-1015 Lausanne, Switzerland

⁴ISDC Data Center for Astrophysics, Center for Astroparticle Physics, Observatory of Geneva, University of Geneva, Chemin d'Ecogia 16, CH-1290 Versoix, Switzerland

⁵Universität Würzburg, Institute for Theoretical Physics and Astrophysics, Emil-Fischer-Str. 31, D-97074 Würzburg, Germany

^aalso at University of Zurich, CH-8057 Zurich, Switzerland

^balso at Kyungpook National University, Center for High Energy Physics, 702-701 Daegu, Korea

^calso at Max-Planck-Institut für Physik, D-80805 Munich, Germany

^dalso at Technische Universität München, D-85748 Garching, Germany

thomas.kraehenbuehl@phys.ethz.ch

DOI: 10.7529/ICRC2011/V09/0529

Abstract: The First G-APD Cherenkov Telescope (FACT) collaboration builds a camera for a Cherenkov Telescope which is based on G-APDs and an integrated digitisation using the Domino Ring Sampling (DRS4) chip. The amplitude calibration must account for a wide variety of effects which are inherent to the chosen design of the camera. G-APDs show a strong temperature dependence, the quality of the glueing of the optical components must be accounted for, and the non-linearities of the signal amplification and the DRS4 chip must be characterized and corrected. The calibration is based on an online feedback system to stabilize the gain of the G-APDs, laboratory measurements and dedicated data-taking runs.

Keywords: Geiger-mode Avalanche Photodiode, Imaging Atmospheric Cherenkov Telescope, Calibration, Domino Ring Sampler, DRS4, FACT

1 Introduction

The field of Imaging Atmospheric Cherenkov Telescopes is still undergoing a rapid development: on the one hand, both hardware and analysis techniques are constantly improved, and on the other hand a large number of discoveries and results reward this constant search for better techniques. A next major step for the field is expected with the Cherenkov Telescope Array (CTA)¹, which promises major sensitivity and resolution improvements.

At the heart of such a telescope is a fast and sensitive camera, which registers the weak Cherenkov flashes of the high energy particles in the atmosphere. The cameras of all current experiments are based on Photomultiplier Tubes (PMT), which is also in the roadmap for CTA [1]. The recent improvements of Geiger-mode Avalanche Photodi-

odes and their commercial availability from several manufacturers have made them an interesting candidate to replace the PMTs in Cherenkov Astronomy. The First G-APD Cherenkov Telescope (FACT) collaboration evaluates the feasibility of those sensors for IACT cameras by building and evaluating a prototype camera, which will be installed in the refurbished HEGRA CT3 telescope on the Roque de los Muchachos on La Palma. More information on the FACT project can be found in [2, 3].

2 A short introduction to G-APDs

Geiger-mode avalanche photodiodes (G-APD) are semiconductor photosensors where the sensitive area is divided

1. <http://www.cta-observatory.org/>

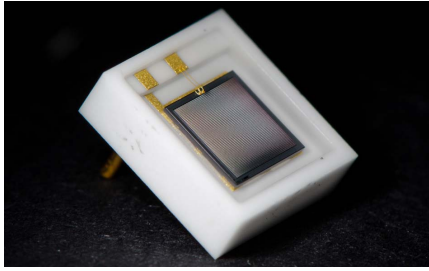


Figure 1: One of the G-APDs of the FACT camera. The sensitive area (black) has a size of $3 \times 3 \text{ mm}^2$.

into cells, each of which operates in Geiger-mode. Each cell can thus only detect one photon at a time, which causes a statistical saturation effect [4]. The single cells are connected in parallel such that the total signal of a G-APD is the analog sum of all cells. Compared to PMTs, G-APDs have a very good single photon resolution in the sense that the signals of one, two or more cells can be well distinguished.

G-APDs have no need for high voltage power supplies and are usually operated below 100 V. The gain is linear to the so-called over-voltage ΔV which is the difference between the bias voltage and the breakdown voltage of the chip. For the G-APDs in the FACT camera (Hamamatsu S10362-33-050C, see figure 1), typical values for the bias voltage are around 70 V, and the over-voltage is $\sim 1.1 \text{ V}$. The breakdown voltage depends on the temperature with a coefficient of about $55 \text{ mV}/^\circ\text{C}$.

Besides the gain, many other properties of the G-APDs depend on the over-voltage. The photon detection efficiency (PDE), ie. the probability that a single photon impinging on the surface triggers a cell, depends exponentially on the over-voltage $\text{PDE} = k(1 - e^{-\alpha\Delta V})$, see eg. [6]. The crosstalk² probability depends on the gain and thus on the over-voltage. Note that the crosstalk probability does not depend on the temperature for a constant gain [7]. See figure 2 for the measured dependencies on the over-voltage.

For more information on G-APDs see e.g. [8, 9].

3 Calibration

The calibration of a Cherenkov telescope camera contains a multitude of measurements. The FACT collaboration groups those measurements according to two criteria: they belong either to the sensor compartment or the electronics of the camera, and the measured property changes on a short- or long-term time-scale. The long-term properties are measured in the laboratory, while the short-term properties are either checked on-line or once per night.

Special attention is paid to the dependence of the G-APD properties on the overvoltage. Since this overvoltage changes not only with temperature but also with the amount of background light, a stabilization system was im-

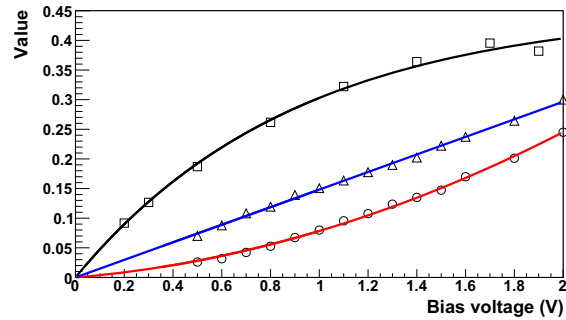


Figure 2: Dependence on the over-voltage of three main parameters: gain (blue, triangles), photon detection efficiency (black, squares) and crosstalk probability (red, circles). Reprinted from [5].

plemented for an online adaptation of the overvoltage (for more details, see section 4).

3.1 Electronics properties: Preamplifier- and digitization linearity

An important property of the preamplifier and digitization electronics is their non-linearity. To measure the characteristic curve "input voltage vs. digitized value" for every readout channel, electronic pulses of varying size over the whole dynamic range were injected into the preamplifiers. For this test, the sensor compartment was not yet connected to the camera. The injected pulses were analyzed, and from the comparison of the pulse size before injection and after the digitization the linearity of the electronics chain was reconstructed. This data will be used in the data analysis to calibrate differences between the electronics channels.

3.2 DRS calibration

The digitization of the signals is based on the Domino Ring Sampling chip (DRS4) [10]. The DRS4 chip contains a ring buffer with 1024 samples for 9 channels, the frequency of the sampling can be adjusted between 700 MHz and 5 GHz. The chip is used at a frequency of 2 GHz in the FACT project.

The ring buffer is built as a chain of capacitors. The signal is fed continuously into the capacitors. After an external trigger (see [11]) the writing is stopped and the capacitors are read one by one and digitized with an external ADC. Each capacitor of the DRS chip has its own offset and gain. In the FACT camera, the uncalibrated data has a RMS in the order of 15 mV (compared to the dynamic range of 2 V). In order to extract the signals of single G-APD cells, which have an amplitude of $\sim 10 \text{ mV}$, it is necessary to correct the

2. Crosstalk in a G-APD means that a cell triggers a neighbouring cell during its breakdown, thus creating a signal which is twice as large (or more for multiple crosstalk cells) as the single cell signal. The crosstalk probability for the FACT G-APDs is 10% at the operation voltage.

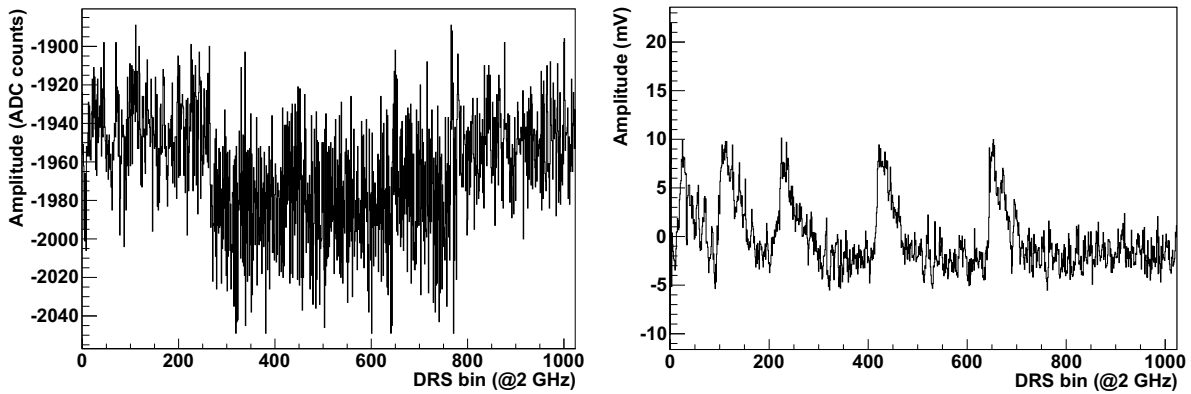


Figure 3: The same event before and after the DRS calibration. After the calibration the pulses corresponding to one single G-APD cell are clearly visible.

offset and gain for every single sampling capacitor. This reduces the RMS to below 2 mV (see figure 3).

3.3 Relative photon detection efficiency

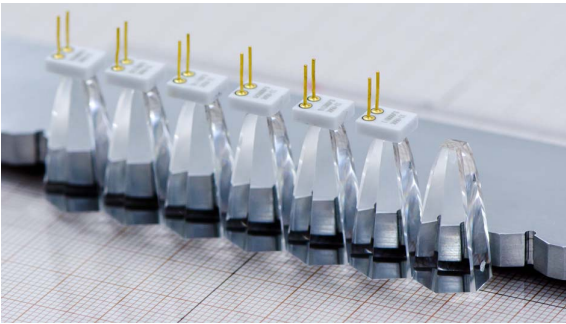


Figure 4: Test glueing of some pixel (consisting of a cone and a G-APD) to a PMMA window. For the alignment, a custom-made ruler is used.

The sensor compartment of the FACT camera is made of three parts: the G-APDs, a light-collecting cone and a PMMA window. The cones are produced by injection molding and concentrate the light from the hexagonal entrance window onto the square exit window on the sensor side. In a first step, 1545 cones were glued to G-APDs. A selection of 1440 pixel was then glued to the entrance window (see figure 4).

An important property of an IACT camera is the homogeneity of the photon detection efficiency over the whole sensor plane. Differences between the pixel can be introduced at every stage of the photon path: the quality of the glueings, the transmission of the cones and the PDE of the G-APDs may vary. The PDE differences are assumed to be much smaller than the other differences and thus neglected. The spectral transmission of every single cone was measured and a cutoff applied (see [12]).

In the glueing process, mainly two problems need special attention: the alignment of the cone on the G-APD and the appearance of bubbles in either of the two glueings. The selection of the pixel to be glued onto the window was mainly based on the amount and size of the bubbles in the glueing. However, it should be noted that even for the worst glueings the light loss due to the bubbles is less than 3% according to a simulation.

To account for these variations between pixel, a relative PDE is introduced. This relative PDE is determined using weak light flashes: for such events, the number of photons on the G-APD is Poisson distributed. The mean number of detected photons μ can be calculated as $\mu = -\ln(N_0/N_{\text{tot}})$, with N_{tot} the total number of events and N_0 the number of events where no photon was detected. This method has the advantage that the result is independent of crosstalk and saturation effects. By comparing the mean number of detected photons across the pixel of the camera, the relative PDE is determined.

4 The feedback system

As described before, most properties of a G-APD change with the over-voltage (see section 2). For the FACT camera design, two processes may change the over-voltage: the operation of the camera under outdoor conditions implies changing ambient temperatures. Furthermore, a serial resistor to the G-APDs in the readout electronics leads to a dependence on the amount of background light: if the field of view of the camera gets darker or brighter, the current in the sensors and thus in the serial resistor changes, which leads to a changing voltage drop over the resistor.

To correct these two effects, a feedback system using a light pulser is implemented. The light pulser emits short light flashes of an adjustable intensity. These pulses are detected by the G-APDs and analyzed to find changes in the pulse size. If necessary, the bias voltage is adapted to

match the pulse size to the expected value. The first tests of this feedback system were made in summer 2009 [13].

The feedback pulser contains an internal temperature stabilization. To check the correct operation of the feedback system, the size of the single cell signals (i.e. the gain) must be checked. This is achieved by analyzing the background noise from night sky photons and G-APD dark counts and extracting the size of single cell signals. Since this analysis is only possible if the background rate is low, the checks will be made in dedicated "dark night runs", where no moon is present.

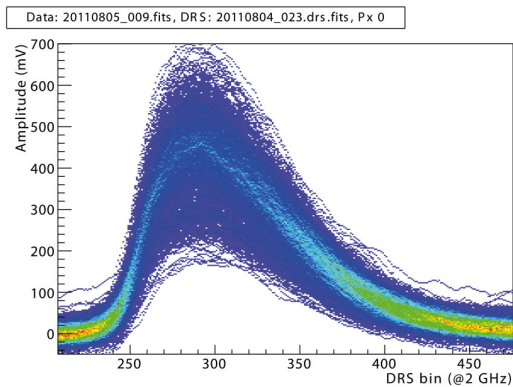


Figure 5: Pulses of the feedback system.

5 Acknowledgements

The important contributions from ETH Zurich grant ETH-10.08-2 as well as the funding of novel photo-sensor research by the German BMBF Verbundforschung are gratefully acknowledged. We also thank the Instituto de Astrofísica de Canarias allowing us to operate the telescope at the Observatorio del Roque de los Muchachos on La Palma, and the Max-Planck-Institut für Physik for providing us with the mount of the former HEGRA CT3 telescope.

References

- [1] The CTA Consortium, Design Concepts for the Cherenkov Telescope Array, arXiv.org (2010).
- [2] A. Biland *et al.*, First Results from the First G-APD Cherenkov Telescope, in these proceedings.
- [3] T. Bretz *et al.*, Status of the First G-APD Cherenkov Telescope (FACT), in these proceedings.
- [4] Hamamatsu Photonics K.K., MPPC datasheet, (2008).
- [5] H. Anderhub *et al.*, Nucl. Inst. Meth. A Vol. 639 Issue 1 (2010) 55-57. doi: 10.1016/j.nima.2010.09.063
- [6] D. Orme *et al.*, Proceedings of Science PoS(PD09)019 (2009).
- [7] Diploma thesis, http://ihp-lx2.ethz.ch/pub/dipl/Dipl_Kraehenbuehl_Thomas.pdf
- [8] D. Renker and E. Lorenz, JINST 4 (2009) P04004.
- [9] T. Kraehenbuehl *et al.*, Proceedings of Science PoS(PD09)024 (2009).
- [10] S. Ritt, Nuclear Science Symposium Conference Record Vol. 2 (2004) 974 - 976.
- [11] P. Vogler *et al.*, Trigger and Data Acquisition electronics for a Geiger-mode avalanche photodiode Cherenkov Telescope Camera, in these proceedings.
- [12] B. Huber *et al.*, Solid light concentrators for small-sized photosensors used in Cherenkov telescopes, in these proceedings.
- [13] H. Anderhub *et al.*, Nucl. Inst. Meth. A Vol. 628 Issue 1 (2011) 107-110. doi: 10.1016/j.nima.2010.06.296